Macromolecular Chemistry and Physics
www.mcp-journal.de

Synthesis of Fluorine-Containing, UV-Responsive PLA-Based Materials by Means of Functionalized DOX Monomer

Stefano Gazzotti, Marco Aldo Ortenzi, Hermes Farina, and Alessandra Silvani*

1,3-Dioxolan-4-ones (DOX) chemistry is exploited for the synthesis of UV-curable, polylactic acid (PLA)-based copolymers. DOX monomer functionalized with 4-fluoro-4′-hydroxybenzophenone is synthesized and employed as comonomer with L-lactide. Copolymerization reactions are performed with different DOX loadings through a solvent-free, metal-catalyzed protocol. Products are characterized through NMR analysis in order to demonstrate the random insertion of the modified monomer within the polymeric chain. Copolymers are subjected to UV irradiation and compared to a control PLA synthesized and processed in the same conditions. The evolution of the molecular weight during prolonged UV exposure is evaluated through SEC analysis, showing the effect of the benzophenone side groups, which promote crosslinking reactions. A crosslinking mechanism is proposed and demonstrated by means of ^{1}H NMR and FT-IR analyses. The gel content of the samples is measured after the UV exposure, demonstrating a correlation with the concentration of DOX-derived units. Finally, water contact angle analyses are performed to investigate the effects of the fluorination degree on the wettability properties and thermal characterization is carried out. Moreover, rheological analyses show a shear thickening behavior for the copolymers with the highest concentration of DOX-derived units.

1. Introduction

Polylactic acid (PLA)-related research is flourishing, pushed forward by the increasing demand of valid solutions for the plastic pollution problem in the world.[1,2] To this regard, highly recyclable materials often represent the best choice in terms of sustainability. On the other hand, biobased and biodegradable polymers are attracting more and more interest, to replace commonly employed oil-derived plastics in many different fields of application.[3] In particular, academic and industrial research often targets polymers with good biodegradability as they would help to limit the accumulation of end-of-life goods in the environment. Within such a class of materials, PLA is one of the most studied and developed since its monomer (i.e., lactic acid) can be extracted from many different natural sources and its degradation products are unharmful for living beings.[4,5] High stiffness, high tensile strength and good optical features of PLA paved the way to a wide span of applications, ranging from food packaging to tissue engineering.[6,7] In particular, employment in the biomedical field has always attracted much interest, thanks to PLA biocompatibility and good processability, which allows for the preparation of scaffolds, even with complex shapes.[8,9] However, PLA's poor toughness has always been a strong hurdle to its applicability in this field, especially when dealing with bone-regeneration applications.[10,11] In the search for possible improvements of PLA's mechanical properties, one of the most investigated approaches relies on the preparation of crosslinked materials, since crosslinks impart additional dimensional stability to the polymer, improving its toughness.[12] They are usually obtained by introducing acrylic moieties that can eventually be UV-cured to yield the crosslinked lattice.[13–15] The strong limit of this approach is related to acrylates toxicity, which makes the obtained material unsuitable for in vivo applications unless thoroughly purified.[16]

Besides poor mechanical properties, PLA's in vivo applicability is often limited by inadequate surface properties and hydrophobicity and low surface energy, as well as the lack of surface functional groups, likely hindering proper cell adhesion.[17,18] A partial fluorination of the surface has been recently reported as a possible improvement, as it was demonstrated that partially fluorinated surfaces can promote the cells' adhesion and proliferation, thanks to the formation of favorable dipoles.[19–21] To this regard, it is important to balance properly the fluorination degree, in order to avoid an increased hydrophobicity that would hinder proper in vivo interactions.[22]

Given these premises and relying on our expertise in the preparation of functional PLAs,[23,24] the synthesis of a curable

S. Gazzotti, M. A. Ortenzi, H. Farina, A. Silvani
Dipartimento di Chimica
Università degli Studi di Milano
Via Golgi 19, Milano 20133, Italy
E-mail: marco.ortenzi@unimi.it
S. Gazzotti, M. A. Ortenzi, H. Farina, A. Silvani
CRC Materiali Polimerici "LaMPo"
Dipartimento di Chimica
Università degli Studi di Milano
Via Golgi 19, Milano 20133, Italy

The ORCID identification number(s) for the author(s) of this article can be found under https://doi.org/10.1002/macp.202100436

DOI: 10.1002/macp.202100436

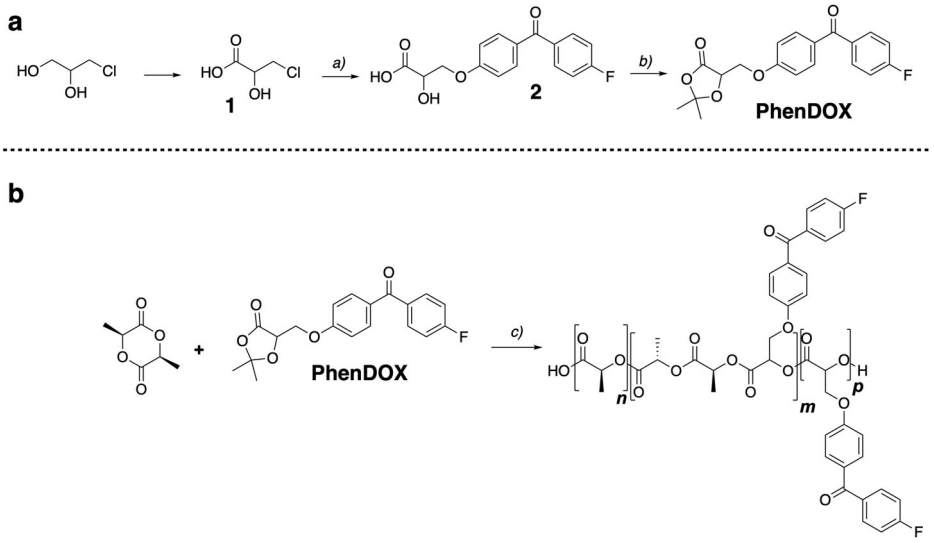

Scheme 1. Synthesis of PhenDOX indicating reagents and conditions (upper scheme) and copolymerization between PhenDOX and L-Lactide (lower scheme). In upper scheme: a) 4-fluoro-4′-hydroxybenzophenone, NaOH, H_2O, reflux, 4 h, 33% yield; b) acetone, H_2SO_4, 4 h, 70% yield. In lower scheme: c) $Zn(ClO_4)_2{\cdot}6H_2O$ (0.25 w/w% with respect to monomers), $Zn(OTf)_2$ (0.05 w/w% with respect to the monomers), $Sn(Oct)_2$ (0.03 w/w% with respect to the monomers), 190 °C, 4 h, under N_2 flow.

PLA-based material, endowed with a tunable degree of fluorine content, was conceived. To the best of our knowledge, no similar polymeric scaffolds have been reported in literature until now. Going on with our recent exploitation of 1,3-dioxolan-4-ones (DOXs) as intriguing monomers for functional PLA synthesis,[25] a new DOX monomer, bearing 4-fluoro-4′-hydroxybenzophenone as side group, was specifically designed in order to guarantee UV light sensitivity for the curing reaction, as well as fluorine presence in the final material. Different than acrylates, benzophenone, and its derivatives are generally considered non-toxic[26,27] and they are often employed as UV absorbers in combination with many different matrices aimed at several different fields of application.[28–30] As the physical mixing of the active benzophenone with the polymeric matrix usually ends up in the loss of activity with time due to diffusion phenomena, and in the loss of mechanical properties due to the presence of a low molecular weight species physically mixed with the polymer, the covalent bond of the functional molecule to the polymeric backbone appears intriguing for such applications.[31–33] Copolymerization of DOX monomer with L-lactide, by means of a previously optimized protocol,[25] was carried out. PLA-based materials bearing fluoro hydroxybenzophenone moieties at different loadings were successfully obtained and characterized, studying the effect of UV exposure on their properties. The strong dependance in UV-sensitivity of the final materials on the amount of loaded benzophenone was determined.

2. Results and discussion

2.1. PhenDOX Synthesis and Polymerization with L-Lactide

The synthesis of 4-fluoro-4′-hydroxybenzophenone-functionalized DOX (PhenDOX) proceeded straightforwardly, without the use of particularly harsh conditions (**Scheme 1a**). PhenDOX was then employed as comonomer with L-lactide for copolymerization reactions. Our recently reported solvent-free, metal-catalyzed protocol for L-lactide-DOX copolymerizations is based on a combination of three different metal catalysts, which proved to be effective for the complete insertion of DOX monomers when low loadings are employed.[25] Copolymerization reactions between PhenDOX and L-lactide were carried out using the same protocol, with PhenDOX loadings ranging from 0.1 to 2 mol/mol%. Briefly, a combination of zinc trifluoro methanesulfonate ($Zn(OTf)_2$), zinc perchlorate hexahydrate ($Zn(ClO_4)_2{\cdot}6H_2O$), and tin(II) 2-ethylhexanoate ($Sn(Oct)_2$) was employed as catalytic system. Copolymerization reactions were performed at 190 °C for 4 h under nitrogen atmosphere, as indicated in the general reaction scheme (Scheme 1b).

DOX polymerization mechanism has been investigated for what regards homopolymerization reactions.[34,35] It has been demonstrated that Lewis acid-catalyzed polymerization involves a cyclic transition state in which the Lewis acid coordinates the DOX's carbonyl and promotes the attack of the nucleophilic species (i.e., the initiator or the growing chain terminal group). The driving force for the reaction is the elimination of the aldehyde or ketone used as the protecting group for the parent α-hydroxy acid. When formaldehyde is employed, the elimination competes with the Tishchenko reaction which results in the formation of acetal bridges that are detrimental for the final properties of the material.[36] The mechanism of DOX polymerization closely resembles the Ring Opening Polymerization (ROP) mechanism of lactones, such as lactide, where the Lewis acid coordinates the carbonyl and catalyzes the chain growth through the release of ring strain.

2.2. Size Exclusion Chromatography (SEC)

All products were analyzed through SEC, in order to determine the effect of different quantities of PhenDOX-derived units on the hydrodynamic volume of the final product. Molecular weight

Table 1. Molecular weight data of the copolymers compared to a standard PLA.

Sample	PhenDOX loading (mol/mol%)[a)]	PhenDOX-derived repeating units (mol/mol%)[b)]	$\overline{M_n}$ [g mol^{-1}][c)]	M_p[g mol^{-1}][c)]	Đ
PLA	0	0	13 300	14 400	1.6
PLA-co-0.1	0.1	n.d.	11 900	12 700	1.6
PLA-co-0.2	0.2	0.1	11 900	13 000	1.8
PLA-co-0.5	0.5	0.2	11 800	13 000	1.7
PLA-co-1.0	1.0	0.4	11 200	12 600	1.8
PLA-co-2.0	2.0	0.9	10 100	11 000	1.7

[a)] Loaded monomer calculated with respect to L-lactide; [b)] Determined via ^{1}H NMR, as ratio between the signal of the aromatic protons at 7.00 ppm and the lactide-derived signal at 5.19 ppm, belonging to the –CH group in the macromolecular chain; [c)] Determined through SEC against a PS calibration. Molecular weights are approximated to one hundred.

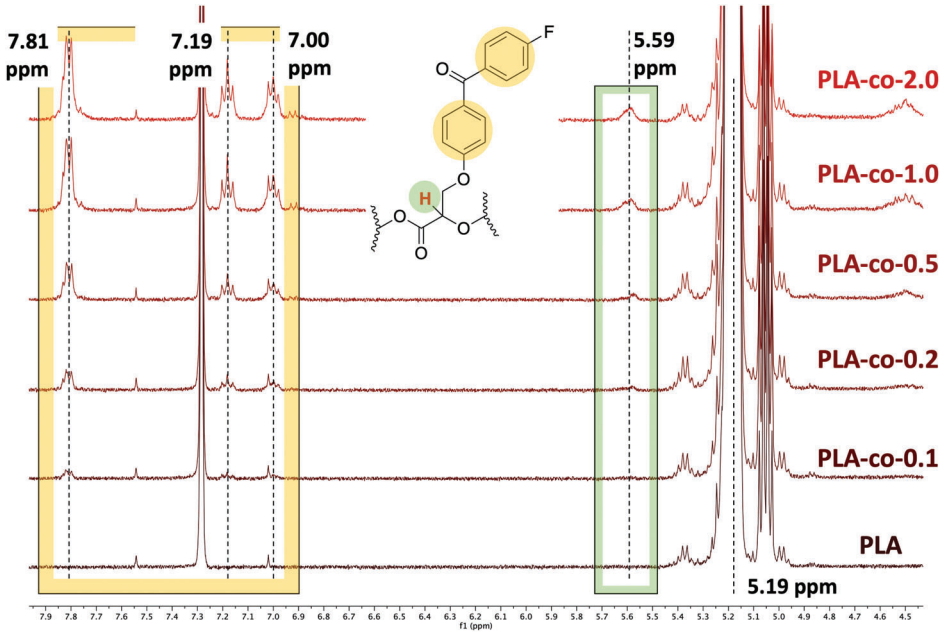

Figure 1. Stacked ^{1}H NMR spectra for all crude samples. Frames highlight the presence of signals attributed to PhenDOX-derived units.

data are reported in **Table 1** and compared to that of a standard PLA synthesized in the same conditions and used as reference.

As Table 1 shows, all copolymers were characterized by a slightly lower hydrodynamic volume with respect to PLA, with the lowest value detected for the PLA-co-2.0 sample. As already reported, with increasing concentration of DOX comonomer in the feed the molecular weight tends to decrease, because of two distinct reasons. From one side, at a relatively high DOX concentration the catalyst loses activity toward polymerization, causing a decrease of monomer conversion. On the other hand, our previous work also demonstrated that DOX monomers partially deprotect before the polymerization takes place, releasing the free α-hydroxy acid which acts as initiator.[25]

2.2.1. H-NMR Analysis

All crude products were characterized through ^{1}H NMR analysis, in order to evaluate the actual insertion of the comonomer in the chains. **Figure 1** reports the stacked spectra for all samples in the 8.0 to 4.5 region.

The predominant signal, which is present in each spectrum at 5.19 ppm, was assigned the CH group of L-lactide-derived units. Except for PLA, all samples show other peaks in the framed regions. At 5.59 ppm the broad peak appearing and increasing in intensity in parallel with PhenDOX loading, is attributable to the CH group of PhenDOX-derived units. This assumption is confirmed by the 2D correlation with the broad CH_2 signal at 4.49 ppm highlighted by the COSY spectrum of PLA-co-2.0 (reported in the SI file). The strong downfield shift of this CH signal can be explained not only by electronic but also steric reasons, being significantly more encumbered with respect to the same proton in lactide-derived units. Similarly, all copolymers show three distinct signals in the aromatic region (7.81, 7.19, and 7.00 ppm), assigned to the 4-fluoro-4′-hydroxybenzophenone side group protons. Signals relative to unreacted DOX are not present in any spectrum according to the ^{1}H NMR of PhenDOX (reported in the Supporting Information file). This observation confirms a full insertion of the monomer and therefore the effi-

ciency of the copolymerization protocol at low DOX loadings. In order to further confirm the reliability of the protocol, the concentration of PhenDOX-derived units in the copolymer was calculated by means of ^{1}H NMR. Integrals of the signals at 7.00 and 5.19 ppm were compared as signals of the PhenDOX-derived units and L-lactide-derived units, respectively, and are results reported in Table 1. As the data show, copolymerization reaction proved to be reliable with full insertion of the loaded DOX. As expected,^{1}H NMR-determined loading is close to the half of the molar loading with respect to L-lactide, since each L-lactide molecule gives two repeating units. The little discrepancies between the theoretical values and the calculated concentrations arise from the integration of the signals that is not always fully reliable given the low concentration of the monomer. This observation is especially true in the case of PLA-co-0.1, where the low intensity of the signals couldn't allow a proper calculation.

When targeting copolymerization reactions involving monomeric systems such as DOX or O-carboxyanhydrides (OCAs), the catalyst exerts a significant effect on the resulting microstructure of the product. Selective catalysts can be exploited for the synthesis of block copolymers, with optimal control on the sequence of repeating units.[37,38] On the other hand, when non-selective catalysts are employed, random copolymers are obtained. As previously reported, using the combination of metal catalysts here described in DOX-lactide copolymerization reactions results in a random distribution of the DOX-derived units along the chain.[25]

2.3. UV Light Exposure

Once the presence of PhenDOX-derived repeating units was demonstrated, copolymers were purified through precipitation, in order to remove all possible unreacted species. Products were then subjected to UV-light irradiation, with the aim of investigating the UV sensitivity of the synthesized species in comparison to a standard PLA. Within this context, the grafting of benzophenone derivatives onto different kinds of polymeric chains have been explored extensively, aimed to either promote photo-induced crosslinking reactions or act as UV adsorbers. Benzophenone-derived units are indeed able to inhibit the photodegradation of the material since UV-light irradiation is able to generate a radical on the carbonyl carbon of benzophenone, which is then transferred to other species. All copolymers were subjected to UV-irradiation for 96 h, taking samples throughout the exposure time and analyzing them through SEC. Samples were taken at 3, 13, 24, 48, and 96 h of exposure and the evolution of $\overline{M_n}$ and Đ was investigated (**Figure 2**).

As expected, in the first stages of UV exposure the PLA sample shows a decrease of the molecular weight, resulting from the light-promoted chain scission phenomena. On the other hand, all the copolymers show an opposite trend, with an increase of molecular weight during the first hours of exposure. This behavior demonstrates the effectiveness of the benzophenone side groups as UV absorbers moieties, preventing the photoaging of the material. Remarkably, this effect was registered in the whole range of tested PhenDOX loadings, showing the potential of this approach even when low concentrations are employed.

In general, all samples show a dependence of the molecular weight evolution with the content of PhenDOX-derived units, with trends closely resembling that of standard PLA when low loadings (0.1 and 0.2 mol/mol%) were employed. On the other side, as expected, higher PhenDOX loadings promote significant changes in the molecular weights with increasing UV-light exposure time compared to PLA.

For PLA-co-0.5, PLA-co-1.0 and PLA-co-2.0, a rapid increase of $\overline{M_n}$ can be detected, starting from the early hours of UV-exposure (Figure 2A). The three samples show a similar trend up to 48 h, while differentiate afterward. $\overline{M_n}$ of PLA-co-0.5 only slightly decreases from 48 to 96 h, while for both PLA-co-1.0 and PLA-co-2.0 it decreases more consistently. This behavior can be explained considering that PLA-co-1.0 and PLA-co-2.0 samples taken at 48 and 96 h were not completely soluble, indicating that gel point has been reached after ≈48 h of UV-irradiation. As a polymer reaches its gel point it becomes insoluble, even at high temperatures. Therefore, the presence of an insoluble fraction in the samples demonstrates the occurrence of light-induced branching reactions, promoted by the benzophenone side units. The more extended is the branching, the tighter will be the intermolecular network, leading to the formation of fully crosslinked regions that are not soluble.[39–41] For this reason, the molecular weight data at 48 and 96 h only refer to the soluble fraction of material that is still below the gel point. PLA-co-0.1 and PLA-co-0.2 show an initial increase of molecular weight as well, but at a lower extent with respect to the other three copolymer samples. Their $\overline{M_n}$ remains almost constant up to 48 h: at higher times a strong increase of molecular weight can be detected for PLA-co-0.2, as if the crosslinking was triggered later, due to a lower concentration of active benzophenone-derived side groups. The evolution of $\overline{M_w}$ is similar to that of $\overline{M_n}$ but, in this case, the increase for PLA-co-2.0 is significantly more pronounced when compared to that of the other copolymers, as shown by the evolution of Đ (Figure 2B). To this regard, the great difference in the evolution of $\overline{M_w}$ for PLA-co-PS-2.0 with respect to the other samples confirms the significantly higher degree of crosslinking occurring for this sample, as the higher concentration of benzophenone units translates into more abundant crosslinking sites. Probably, at 48 h of exposure, high branching is occurring, ultimately leading to crosslinking, and this turns into high dispersity values of the sample.

Once the increase of molecular weights, promoted by 4-fluoro-4′-hydroxybenzophenone-derived side groups through UV-irradiation, was demonstrated, the chemical nature of the crosslinking was investigated by means of NMR analysis. PLA-co-2.0 was chosen as reference copolymer since, according to SEC analysis, it shows the most significant transformation. **Figure 3**A reports the^{1}H NMR spectrum of purified PLA-co-2.0, compared to that of PLA-co-2.0 after 96 h of UV-irradiation.

As already discussed,^{1}H NMR spectra of all copolymers are characterized by a signal at 5.59 ppm, attributable to the methine proton in Phen-DOX-derived units. As shown in Figure 3A, this signal, well visible in the^{1}H NMR of PLA-co-2.0, is not detectable anymore after 96 h of UV-exposure. Regarding the aromatic region, the^{1}H NMR of PLA-co-2.0 is characterized by the presence of a well-resolved spin system accounting for the eight aromatic hydrogens of the fluoro-benzophenone moiety. This same region becomes scarcely defined after the UV-light

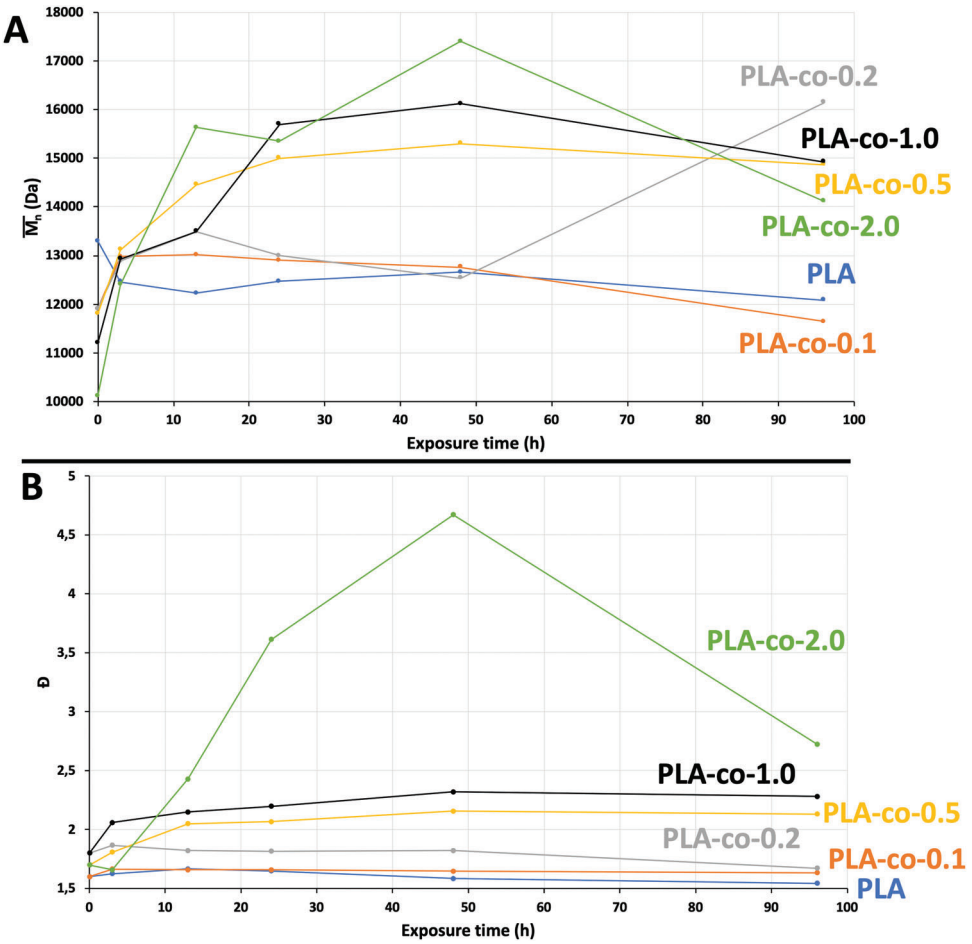

Figure 2. Evolution of A) $\overline{M_n}$, and B) Đ, as function of UV-light exposure time.

treatment, suggesting the active participation of the PhenDOX-derived units to the curing reaction. Hence, relying on the well-known mechanism of benzophenone light-induced activation, a pathway for the crosslinking reaction was proposed (Figure 3B).[42] Under UV-light irradiation, radical species are generated from the PhenDOX-derived units, which are able to promote proton abstraction from the polyester chains. To this regard, the disappearance of the methine signal in the PhenDOX-derived units after UV-exposure suggests that the proton abstraction mainly occurs at that position. Very likely, also the less hampered methine from the lactide-derived units would be involved in the crosslinking, although there is no appreciable variation of the signal at 5.19 ppm, given its high intensity. The crosslinked structure was finally achieved through radical recombination.

In order to further confirm the crosslinking mechanism, FT-IR analysis was performed. **Figure 4** reports the FT-IR spectra of standard PLA and of PLA-co-2.0, in comparison with those resulting after the 96 h of UV-exposure, as well as the magnification of the 1900 to 1550 cm^{-1} range.

The main difference between the spectra of PLA and of PLA-co-2.0 is represented by two bands, at 1602 and 1658 cm^{-1}, respectively, which are present only in the copolymer spectrum. The first one is typical of C=C stretching in aromatic systems conjugated with a carbonyl moiety, while the band at 1658 cm^{-1} is attributable to the stretching of the benzophenone carbonyl group. As Figure 4B shows, no significant differences are detectable for PLA sample before and after the UV-exposure. On the other hand, the IR spectrum of PLA-co-2.0 after 96 h of UV-exposure shows the complete disappearance of the two bands at 1602 and 1658 cm^{-1}, as reported in Figure 4A. This change accounts for a reaction occurring at the carbonyl of the benzophenone moiety. In particular, the carbonyl reacts through a radical mechanism, as described in Figure 3, ending up in the loss of conjugation with the aromatic system and turning out in the disappearance of both the IR key bands. In addition, differences can be spotted regarding the carbonyl stretching band, centered at 1750 cm^{-1}. In the case of PLA the band appears sharper and its shape doesn't change significantly after the UV exposure. PLA-co-2.0 shows a broader band, with a shoulder generated by the stretching of DOX-derived carbonyl groups which decreases in intensity after the curing process as highlighted by the arrow in the expansion in Figure 4A.

The gel content of all samples after UV-exposure was calculated, through evaluation of the insoluble fraction, in order to determine the extent of the UV-promoted crosslinking (**Table 2**).

As expected, the gel content is directly related to the concentration of PhenDOX-derived units, as it increases with the increasing concentration of UV-sensitive sites.

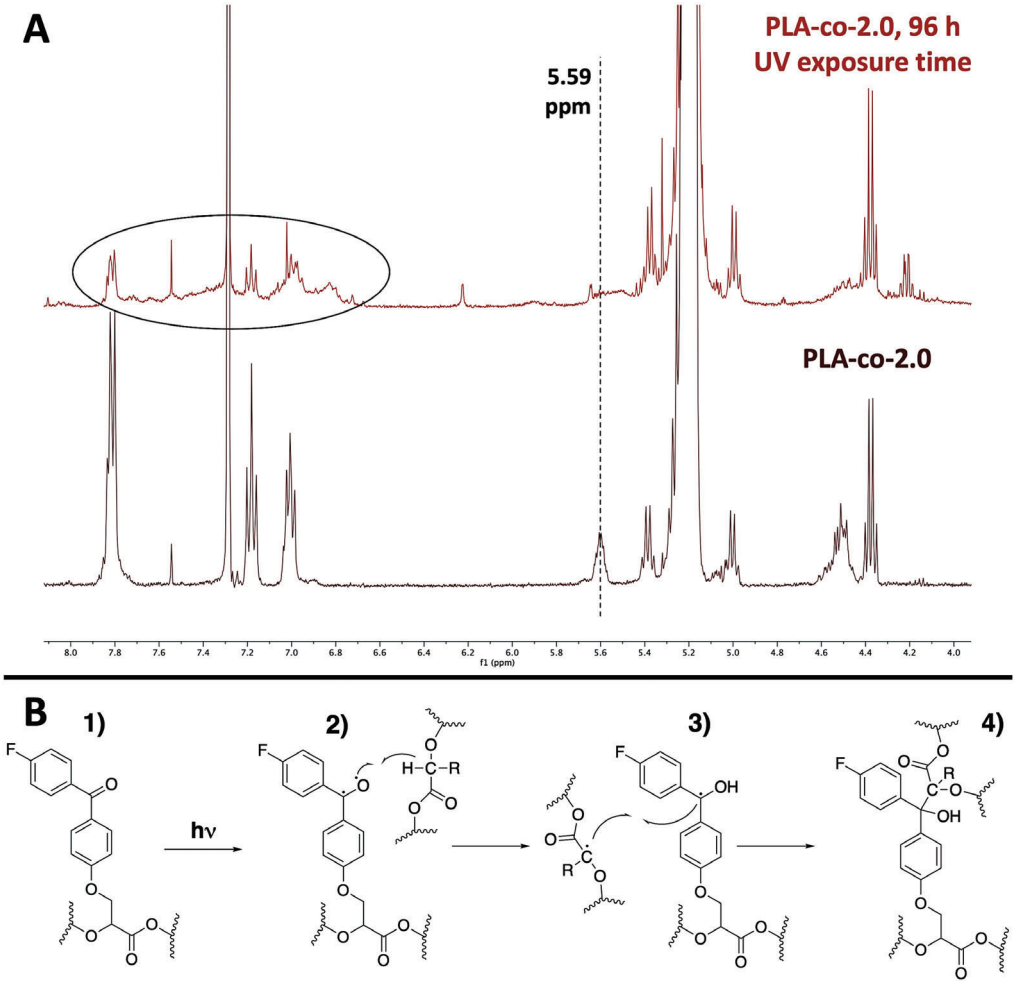

Figure 3. A) Stacked ^{1}H NMR spectra of purified PLA-co-2.0 and PLA-co-2.0 after 96 h of UV-exposure. B) Proposed UV-promoted mechanism.

2.4. Water Contact Angle Analysis (WCA)

Water contact angle analyses were carried out in order to determine the effects of fluorine atoms on the wettability of the materials prior to UV exposure. Films were prepared through solvent casting from a dichloromethane solution. Since it was not possible to form films directly from the synthesized polymers due to their low molecular weight, they were solution blended in a 70 to 30 w/w% ratio with a commercial grade PLA (Natureworks Ingeo 3251D), that is, 70% copolymer and 30% Ingeo 3251D. In order to avoid any possible problem arising from phase separation phenomena given by the polymers' miscibility and the evaporation of the solvent, films surfaces were analyzed before the analyses through FTIR. The two surfaces of the films were compared and no significant differences were detectable. In addition, five different measurements were recorded for each sample in different regions of the surface in order to account for any possible difference in terms of surface composition. Water contact angle results are reported in **Table 3**.

It is well known that the presence of fluorine has profound effects on the wettability properties of the material. On a general level, high fluorination degrees give hydrophobic and even superhydrophobic superficial features, coupled with overall chemical inertness and resistance. However, partial fluorination of surfaces can also be exploited to improve the wettability properties since C-F bonds are characterized by a strong dipole that can increase the surface polarity.[21] In addition, it was demonstrated that partially fluorinated materials can display improved cell adhesion properties, which is a key element for specific in vivo applications.[19,20,43,44] To this regard, it is important to preserve the surface wettability as highly hydrophobic materials would hinder a proper interaction with the growing cells. Fluorine content in the tested blends has been determined and reported in Table 3. Calculations were made based on the actual concentration of PhenDOX-derived units determined through ^{1}H NMR reported in Table 1. As the data show, wettability properties appear to be scarcely influenced by the concentration of PhenDOX-derived units in the copolymer. The surface of the films appeared to be slightly more hydrophobic than standard PLA both in the case of PLA-co-0.1 and PLA-co-0.2. Increasing the loading of DOX monomer ended up in a more hydrophilic material with a decrease of the water contact angle to a minimum of 67.6° for PLA-co-0.5. Finally, PLA-co-2.0 shows similar wettability properties to the standard PLA, despite having the highest concentra-

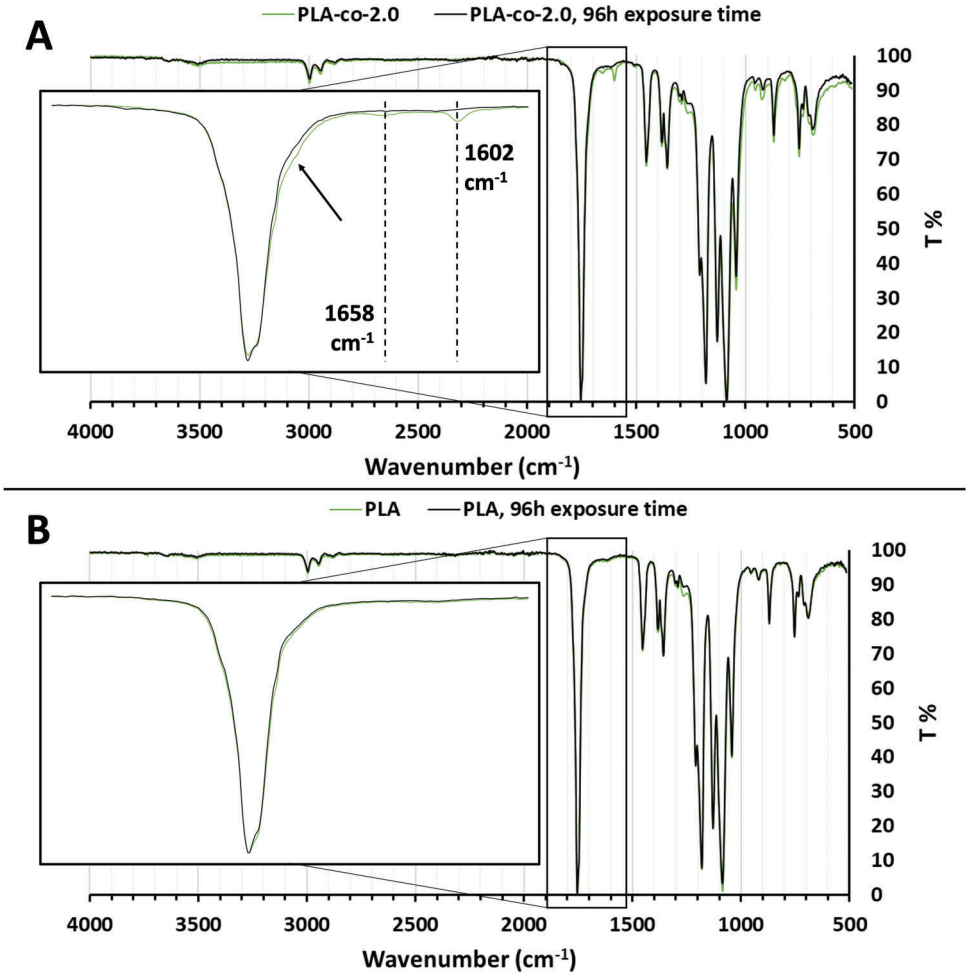

Figure 4. A) Superimposed spectra of PLA-co-2.0 and PLA-co-2.0 after 96 h exposure with expansion in the 1900–1550 cm^{-1}. B) Superimposed spectra of PLA and PLA after 96 h exposure with expansion in the 1900–1550 cm^{-1}.

Table 2. Gel content measured after 96 h of UV-exposure.

Sample	Gel content (w/w)
PLA	1%
PLA-co-0.1	2%
PLA-co-0.2	3%
PLA-co-0.5	16%
PLA-co-1.0	20%
PLA-co-2.0	30%

Table 3. WCA values for all synthesized polymers and fluorine content in each blend.

Sample	Water contact angle [°]	Parts per million of fluorine in the blend
PLA	72 ± 0.2	0
PLA-co-0.1	75 ± 2.7	n.d.
PLA-co-0.2	76 ± 3.4	185
PLA-co-0.5	66 ± 2.5	370
PLA-co-1.0	70 ± 0.8	741
PLA-co-2.0	73 ± 2.6	1672

tion of fluorine-bearing benzophenone side groups among the tested samples. The wettability properties of a material can be influenced by several different factors, both due to chemical composition and physical appearance. Therefore, the negligible differences existing in the water contact angle values between PLA and PLA-co-2.0 could arise from the differences in the chemical nature of the two specimens, as well as physical differences in films (i.e., surface roughness and/or porosity) and not only from the concentration of fluorine atoms in the copolymers. From one side, the lower molecular weight of PLA-co-2.0 with respect to PLA would imply a higher concentration of polar chain ends that would eventually result in a more polar surface and lower water contact angle. On the other hand, the increasing concentration of benzophenone side units results in a higher number of aromatic moieties that would contribute to give the final material a more hydrophobic nature. Remarkably, even at the highest concentration of fluorine in PLA-co-2.0, all the tested materials showed wettability properties close to the ones of pristine PLA,

Table 4. Thermal transitions and thermal degradation data for all synthesized samples.

Sample	T_g [°C]	T_{cc} [°C]	T_m [°C]		$T_{5\%}$ [°C]	$T_{50\%}$ [°C]	$T_{90\%}$ [°C]
PLA	54.3	101.1	156.4		243	285	310
PLA-co-0.1	54.5	100.4	155.9		244	289	315
PLA-co-0.2	54.7	103.9	155.8		247	290	316
PLA-co-0.5	55.2	100.7	153.7	159.5	243	286	308
PLA-co-1.0	54.7	105.7	151.8	157.5	249	289	310
PLA-co-2.0	45.6	100.1	133.6	144.0	154	278	295

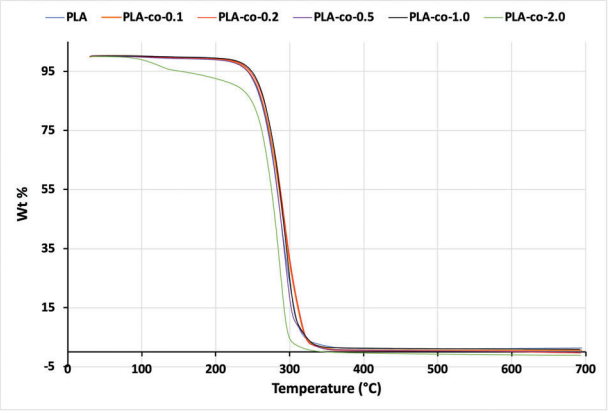

Figure 5. TGA curves for all synthesized samples.

despite the presence of C–F bonds that could have a beneficial effect when looking for in vivo applications (**Table 4**).

2.5. Thermal Analysis

Differential scanning calorimetry (DSC) and thermogravimetric analysis (TGA) analyses were also performed in order to determine the influence of the benzophenone-derived side groups on the thermal properties of the synthesized copolymers. All thermal analyses were performed on the materials before the UV curing. Table 4 reports the thermal data for all samples, with T_g, T_{cc} and T_m referring to glass transition, cold crystallization and melting temperatures recorded during the DSC second heating scan, while $T_{5\%}$, $T_{50\%}$ and $T_{90\%}$ are the degradation temperatures associated to the 5%, 50% and 90% weight losses. DSC thermograms are reported in the Supporting Information file, while TGA degradation curves are reported in **Figure 5**.

The thermal behavior of the samples appears to be strongly influenced by the increasing concentration of DOX-derived repeating units. Glass transition temperatures (T_g) are kept in the same range for all samples with the exception of PLA-co-2.0, which displays a lower T_g with respect to other copolymers. This difference may arise from two distinct aspects: one is due to the racemic nature of PhenDOX; that implies a higher quantity of stereochemically random units present in the final macromolecules with a consequent increase in the overall disorder of the polymer, leading to broader transitions. On the other side, also the lower molecular weight of PLA-co-2.0 with respect to the other samples must be taken into account, prevailing over the increased stiffness given by the aromatic side groups that have the tendency to increase glass transition temperature. Probably, being the molecular weight of PLA-co-2.0 which is quite close to the entanglement molecular weight (M_e) of PLA, that is ≈8700 g mol^{-1},[45] a high quantity of macromolecules in the samples is below the M_e value thus increasing chain mobility and therefore lowering T_g. In the other samples, M_n values are higher and therefore less macromolecules contribute to the high chain mobility. All samples show similar cold crystallization temperatures, while melting behavior changes significantly. To this regard, copolymers with the higher concentration of DOX-derived units (i.e., PLA-co-0.5, PLA-co-1.0, and PLA-co-2.0) are characterized by a double melting peak, denouncing the presence of two distinct crystalline phases. Such a behavior was already described for similar copolymers and it was attributed to the increased disorder promoted by both the bulkiness and the racemic nature of DOX-derived units.[25] In addition, PLA-co-2.0 melting transition occurs at lower temperatures when compared to other samples. This behavior was attributed not only to the high concentration of benzophenone side groups, but also to the low molecular weight of the polymer, which can have detrimental effects on the thermal transitions of the polymer as already discussed regarding the glass transition temperature.

As TGA analyses pointed out all samples show similar thermal degradation behavior, with a single step degradation pathway and similar $T_{5\%}$, $T_{50\%}$ and $T_{90\%}$ as reported in Figure 5. The only sample outside this trend is PLA-co-Phen2.0, showing lower degradation temperatures and a two steps degradation profile likely due to its low molecular weight and higher concentration of DOX-derived units that can promote radical chain scission mechanisms.

2.6. Rheological Analysis

Finally, rheological analyses were performed, in order to evaluate the effects of the varying concentration of benzophenone side groups on the melt viscosity properties of the materials. Complex viscosity curves for PLA, PLA-co-0.2, PLA-co-1.0, and PLA-co-2.0 are reported in **Figure 6**: samples were chosen to better highlight the differences in behavior depending on the concentration of DOX-derived units.

On a general level, all samples showed low viscosities, due to the low molecular weights. However, a strong dependance of the melt viscosity properties on the concentration of DOX-derived units in the copolymer was highlighted. In particular, PLA and PLA-co-0.2 showed similar behaviors, with an overall low

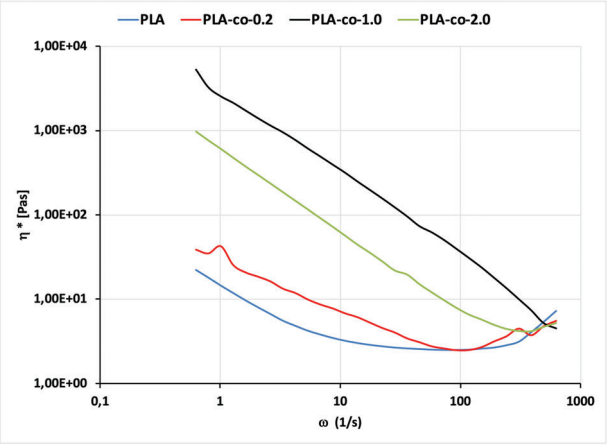

Figure 6. Complex viscosity curves for PLA, PLA-co-0.2, PLA-co-1.0, and PLA-co-2.0.

complex viscosity, increasing toward lower angular frequencies. Despite a lower molecular weight with respect to PLA, PLA-co-0.2 showed a slightly higher viscosity, likely because of the stiffening effect exerted by the aromatic substituents. This effect was more pronounced in the case of PLA-co-1.0 and PLA-co-2.0, where the higher concentration of benzophenone side groups resulted in an overall higher viscosity and strong shear thickening behavior that at low frequencies becomes quite high. Alongside the presence of bulky and rigid benzophenone substituents, also the decrease of molecular weight played a role, resulting in a lower η^* for PLA-co-2.0 in comparison to PLA-co-1.0.

3. Conclusions

In conclusion, the synthesis of a novel monomer for the preparation of fluorine-containing, UV-curable PLA based materials is presented. A 4-fluoro-4′-hydroxybenzophenone containing DOX monomer was synthesized effectively and employed for the preparation of copolymers, together with L-lactide. Different PhenDOX loadings were tested, ranging from 0.1 mol% to 2.0 mol% with respect to L-lactide. The copolymerization reaction was carried out through a solvent-free, metal catalyzed protocol that has allowed a full insertion of the functionalized DOX monomer along the polyester chain. All copolymers were purified through precipitation and their behavior under UV-light irradiation was studied in comparison with that of a standard PLA, synthesized in the same conditions. The evolution of the molecular weight was followed by SEC analysis, which highlighted the increase of $\overline{M_n}$ and $\overline{M_w}$ with UV-exposure time, on a greater extent as the loading of PhenDOX was higher.PLA-co-2.0 showed the greatest increase of molecular weight among all samples, while copolymers with lower loading of benzophenone-derived units proved to be effective in preventing the photodegradation phenomena. From ^{1}H NMR and FT-IR analyses of PLA-co-2.0, before and after the UV-exposure, the actual occurrence of a crosslinking process was assessed. A mechanism for the crosslinking reaction was proposed, taking into account the light-induced activation mode for benzophenone. The gel content after the UV-exposure was measured for all the synthesized copolymers together with water contact angle measurements. Within this context, the possibility to tune the fluorination degree without affecting significantly the wettability properties, coupled with UV-curing capabilities makes these materials valuable for the preparation of scaffolds with in vivo applicability. To this regard, PLA has been widely studied for these applications. The work here presented provides a synthetic strategy to modified monomers that could be exploited for the preparation of functionalized PLA-based materials with different properties depending on the specific targeted final application. On a general level, the insertion of benzophenone derivatives is useful to confer UV-resistance to the material, which is an often-sought property usually achievable with specific additives.[46] Moreover, the occurrence of crosslinking after the UV exposure gives the final copolymers an additional 3D stability that could eventually be beneficial for the preparation of scaffold for biomedical applications.[47] In addition, the use of benzophenones with different substituents could be relevant for the modification of the surface properties of the materials and therefore improve the compatibility with biological media. As a consequence, the presented strategy can serve as a starting point for future investigations with targeted functionalizations depending on the desired final applications. Thermal analyses were performed highlighting a dependence on the amount of loaded DOX monomer. To this regard, the high concentration of DOX-derived units has strong effects on the melting transitions of the polymers, while glass transition and cold crystallization weren't significantly affected. Similarly, thermal degradation behavior was evaluated and all samples showed superimposable degradation curves. The copolymer carrying the highest concentration of DOX-derived units showed different behaviors both in the case of DSC and TGA, likely because of its low molecular weight as well as high amount of benzophenone side-groups. Finally, rheological analyses were performed. Complex viscosity curves showed a dependance of the melt viscosity properties on the amount of aromatic side groups in the copolymers. In particular, samples with the highest concentration of DOX-derived units showed a strong shear thickening behavior, likely resulting from the rigid nature of the substituents.

Supporting Information

Supporting Information is available from the Wiley Online Library or from the author.

Acknowledgements

Open Access Funding provided by Universita degli Studi di Milano within the CRUI-CARE Agreement.

Conflict of Interest

The authors declare no conflict of interest.

Data Availability Statement

The data that support the findings of this study are available from the corresponding author upon reasonable request.

Received: November 19, 2021
Revised: May 16, 2022
Published online: June 17, 2022

[1] A. C. Albertsson, M. Hakkarainen, *Science* **2017**, *358*, 872.
[2] N. Tripathi, M. Misra, A. K. Mohanty, *ACS Eng. Au* **2021**, *1*, 7.
[3] M. Häußler, M. Eck, D. Rothauer, S. Mecking, *Nature* **2021**, *590*, 423.
[4] S. T. Sikhosana, T. P. Gumede, N. J. Malebo, A. O. Ogundeji, *eXPRESS Polym. Lett.* **2021**, *15*, 568.
[5] N. A. Rosli, M. Karamanlioglu, H. Kargarzadeh, I. Ahmad, *Int. J. Biol. Macromol.* **2021**, *187*, 732.
[6] Y. Yang, M. Zhang, Z. Ju, P. Y. Tam, T. Hua, M. W. Younas, H. Kamrul, H. Hu, *Text. Res. J.* **2021**, *91*, 1641.
[7] S. Sharma, *Polylactic Acid (PLA) and Its Composites: An Eco-friendly Solution for Packaging*, Sustainable Food Packaging Technology, Wiley-VCH Ghmb, Wenheim, Germany **2021**, pp. 107–132.
[8] V. A. Marcatto, G. S. Pegorin, G. F. Barbosa, R. D. Herculano, N. B. Guerra, *J. Appl. Polym. Sci.* **2022**, *139*, 51728.
[9] M. Młotek, A. Gadomska-Gajadhur, A. Sobczak, A. Kruk, M. Perron, K. Krawczyk, *Appl. Sci.* **2021**, *11*, 1815.
[10] X. Zhou, G. Zhou, R. Junka, N. Chang, A. Anwar, H. Wang, X. Yu, *Colloids Surf., B* **2021**, *197*, 111420.
[11] J. Lee, H. Lee, K. H. Cheon, C. Park, T. S. Jang, H. E. Kim, H. D. Jung, *Addit. Manuf.* **2019**, *30*, 100883.
[12] P. K. Kuroishi, K. R. Delle Chiaie, A. P. Dove, *Eur. Polym. J.* **2019**, *120*, 109192.
[13] D. K. Han, J. A. Hubbell, *Macromolecules* **1997**, *30*, 6077.
[14] F. P. W. Melchels, J. Feijen, D. W. Grijpma, *Biomaterials* **2009**, *30*, 3801.
[15] J. E. L. Ivirico, M. Salmerón-Sánchez, J. L. G. Ribelles, M. M. Pradas, *Colloid Polym. Sci.* **2009**, *287*, 671.
[16] M. M. Tarskikh, *Bull. Exp. Biol. Med.* **2006**, *142*, 690.
[17] N. De Geyter, R. Morent, T. Desmet, M. Trentesaux, L. Gengembre, P. Dubruel, C. Leys, E. Payen, *Surf. Coat. Technol.* **2010**, *204*, 3272.
[18] H. Xu, M. Shen, H. Shang, W. Xu, S. Zhang, H. - R. Yang, D. Zhou, M. Hakkarainen, *Ind. Eng. Chem. Res.* **2021**, *60*, 12021.
[19] M. Schroepfer, F. Junghans, D. Voigt, M. Meyer, A. Breier, G. Schulze-Tanzil, I. Prade, *ACS Omega* **2020**, *5*, 5498.
[20] R. Khalifehzadeh, W. Ciridon, B. D. Ratner, *Acta Biomater.* **2018**, *78*, 23.
[21] S. Lee, J.-S. Park, T. R. Lee, *Langmuir* **2008**, *24*, 4817.
[22] J. J. Reisinger, M. A. Hillmyer, *Prog. Polym. Sci.* **2002**, *27*, 971.
[23] S. Gazzotti, S. A. Todisco, C. Picozzi, M. A. Ortenzi, H. Farina, G. Lesma, A. Silvani, *Eur. Polym. J.* **2019**, *114*, 369.
[24] S. Gazzotti, M. Hakkarainen, K. H. Adolfsson, M. A. Ortenzi, H. Farina, G. Lesma, A. Silvani, *ACS Sustainable Chem. Eng.* **2018**, *6*, 15201.
[25] S. Gazzotti, M. A. Ortenzi, H. Farina, M. Disimino, A. Silvani, *Macromolecules* **2020**, *53*, 6420.
[26] B. Bandgar, B. Hote, R. Gangwal, A. Sangamwar, *Med. Chem. Res.* **2012**, *21*, 3177.
[27] M. C. Rhodes, J. R. Bucher, J. C. Peckham, G. E. Kissling, M. R. Hejtmancik, R. S. Chhabra, *Food Chem. Toxicol.* **2007**, *45*, 843.
[28] K. H. Hong, N. Liu, G. Sun, *Eur. Polym. J.* **2009**, *45*, 2443.
[29] Z. Huang, A. Ding, H. Guo, G. Lu, X. Huang, *Sci. Rep.* **2016**, *6*, 25508.
[30] J.-D. Cho, S.-G. Kim, J.-W. Hong, *J. Appl. Polym. Sci.* **2006**, *99*, 1446.
[31] F. Ge, Y. Ding, L. Yang, Y. Huang, L. Jiang, Y. Dan, *RSC Adv.* **2015**, *5*, 70473.
[32] O. Prucker, C. A. Naumann, J. Rühe, W. Knoll, C. W. Frank, *J. Am. Chem. Soc.* **1999**, *121*, 8766.
[33] M. Körner, O. Prucker, J. Rühe, *Macromolecules* **2016**, *49*, 2438.
[34] S. A. Cairns, A. Schultheiss, M. P. Shaver, *Polym. Chem.* **2017**, *8*, 2990.
[35] Y. Xu, M. R. Perry, S. A. Cairns, M. P. Shaver, *Polym. Chem.* **2019**, *10*, 3048.
[36] R. T. Martin, L. P. Camargo, S. A. Miller, *Green Chem.* **2014**, *16*, 1768.
[37] X. Wang, A. L. Chin, J. Zhou, H. Wang, R. Tong, *J. Am. Chem. Soc.* **2021**, *143*, 16813.
[38] Q. Feng, R. Tong, *J. Am. Chem. Soc.* **2017**, *139*, 6177.
[39] F. Teymour, J. D. Campbell, *Macromolecules* **1994**, *27*, 2460.
[40] D. R. Miller, C. W. Macosko, *Macromolecules* **1978**, *11*, 656.
[41] A. Ghielmi, S. Fiorentino, G. Storti, M. Morbidelli, *J. Polym. Sci., Part A: Polym. Chem.* **1998**, *36*, 1127.
[42] G. Becker, Z. Deng, M. Zober, M. Wagner, K. Lienkamp, F. R. Wurm, *Polym. Chem.* **2018**, *9*, 315.
[43] C. M. González-Henríquez, F. E. Rodriguez-Umanzor, J. Almagro-Correa, M. A Sarabia-Vallejos, E. Martínez-Campos, M. Esteban-Lucía, A. del Campo-García, J. Rodríguez-Hernández, *Mater. Sci. Eng.: C* **2020**, *114*, 111031.
[44] Z. Qiao, D. Xu, Y. Yao, S. Song, M. Yin, J. Luo, *Polym. Int.* **2019**, *68*, 1361.
[45] J. R. Dorgan, J. S. Williams, D. N. Lewis, *J. Rheol.* **1999**, *43*, 1141.
[46] S. Qiu, J. Sun, H. Li, X. Gu, B. Fei, S. Zhang, *Polym. Degrad. Stab.* **2022**, *196*, 109831.
[47] V. Kudryavtseva, K. Stankevich, A. Gudima, E. Kibler, Y. Zhukov, E. Bolbasov, A. Malashicheva, M. Zhuravlev, V. Riabov, T. Liu, V. Filimonov, G. Remnev, H. Klüter, J. Kzhyshkowska, S. Tverdokhlebov, *Mater. Des.* **2017**, *127*, 261.

